Open Access Full Text Article

ORIGINAL RESEARCH

Uncovering the Mechanisms of BaBaoWuDanYaoMo Against Influenza A Virus and Virus-Induced Inflammation Based on Network Pharmacology and Pharmacological Evaluation

Biao Lei [iD][1,*], Yongjie Su[1,*], Ruihan Chen[1,*], Zexing Chen[1,*], Bin Liu[1], Yuou Chen[1,2], Meihua Zhou[1], Xinhua Wang[1,3], Qinhai Ma[1]

[1]State Key Laboratory of Respiratory Disease, National Clinical Research Center for Respiratory Disease, Guangzhou Institute of Respiratory Health, The First Affiliated Hospital of Guangzhou Medical University, Guangzhou Medical University, Guangzhou, Guangdong, People's Republic of China; [2]King Med School of Laboratory Medicine, Guangzhou Medical University, Guangzhou, Guangdong, People's Republic of China; [3]Institute of Integration of Traditional and Western Medicine, Guangzhou Medical University, Guangzhou, People's Republic of China

*These authors contributed equally to this work

Correspondence: Qinhai Ma; Xinhua Wang, The First Affiliated Hospital of Guangzhou Medical University, Guangzhou, Guangdong, People's Republic of China, Email 13268268214@163.com; xinhuaw@gzhmu.edu.cn

Purpose: The pro-inflammatory response triggered by influenza viruses can contribute to viral pneumonia, even death. The effect and mechanism of BaBaoWuDanYaoMo (BB) against influenza virus remains obscure. To predict its therapeutic targets via network pharmacology and verify the therapeutic effect and the mechanism of BB against influenza virus in vitro and in vivo.

Material and Methods: The potential active and underlying mechanism of BB in the treatment of influenza virus was predicted through network pharmacological strategies and Molecular Docking. The protective and anti-inflammatory effects of BB were determined by cytopathic effect (CPE), quantitative real-time PCR, mitochondrial membrane potentials and Western blotting assay in vitro. BALB/c mice were intranasally infected with A/PR/8/34 (H1N1) (PR8) and orally administrated BB (500 mg/kg, 250 mg/kg and 125 mg/kg) or oseltamivir daily. The normal group was orally administrated PBS for 5 days. Lung indexes, histological changes and cytokines were determined on the 6th day.

Results: BB could effectively inhibit A/Puerto Rico/8/1934 (H1N1), A/GZ/GIRD07/09 (H1N1), A/HK/Y280/97 (H9N2) and A/Aichi/68 (H3N2) with IC_{50} values of 116.5 ± 2.2, 59.86 ± 8.33, 102.87 ± 6.66 and 66.43 ± 6.785 μg/mL, respectively. It could inhibit PR8-induced apoptosis and inhibit the expression of apoptosis markers (cleaved PARP). BB inhibited the mRNA expression of MCP-1/CCL-2, IL-6, CXCL-8/IL-8, TNF-α and CXCL-10/IP-10, and downregulated the protein expression of phosphorylated AKT/p38 and TLR3 in vitro. BB (500 and 250 mg/kg) could improve pulmonary histopathological changes, decrease the lung index and suppress the mRNA expression of CXCL1/KC, TNF-α, CXCL9/MIG and IL-1β in vivo.

Conclusion: BB has a protective effect on PR8-induced acute lung injury (ALI) probably via inhibition of apoptosis process and interfering with TLR3, p38 MAPK and PI3K-AKT signaling pathways. This study provided a potential treatment for influenza from BB, and network pharmacology provided a strategy to explore active components and mechanism of TCMs against influenza virus infection.

Keywords: influenza, apoptosis, viral pneumonia, acute infectious respiratory disease, traditional Chinese medicines

Introduction

Influenza virus, characterized by high contagiousness and rapid spread, can cause substantial disease burden around the world. Influenza A virus is the main subtype that circulates among people and causes epidemics or pandemics.[1] Four

Graphical Abstract
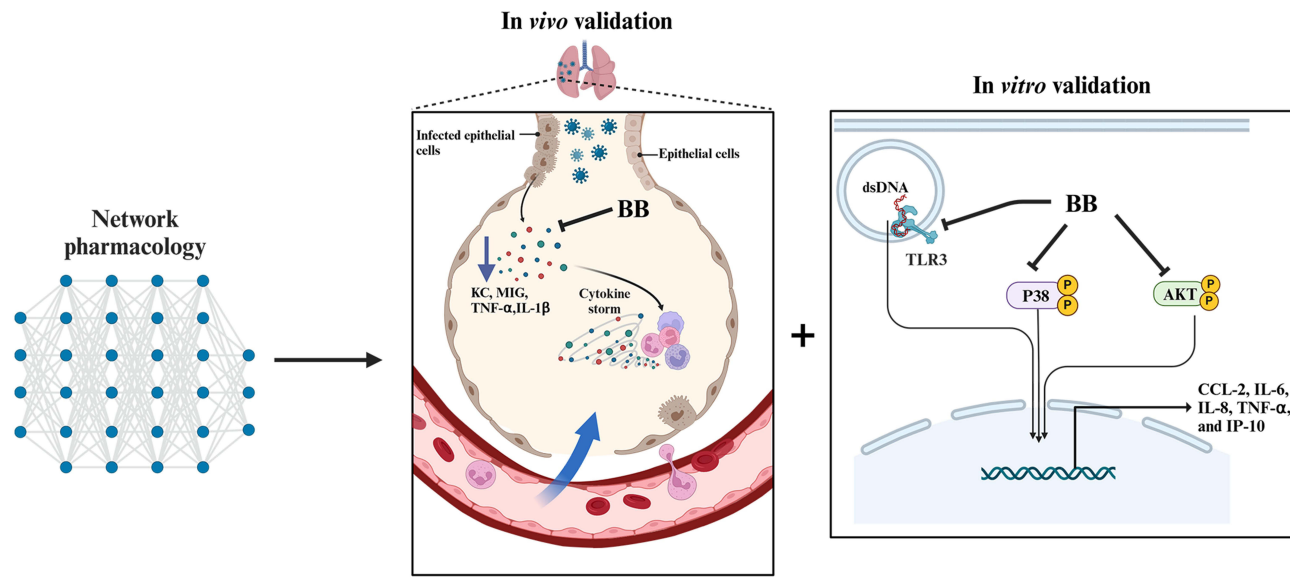
pandemics of human influenza A virus, including H1N1 Spanish influenza in 1918, H2N2 Asian influenza in 1957, H3N2 hong Kong influenza in 1968, and H1N1 swine influenza in 2009, have occurred since the 20th century. The most devastating pandemic, the Spanish influenza in 1918, has caused more than 50 million deaths.[2] Infection with influenza can range from asymptomatic to severe. Uncomplicated influenza can be recovered from easily, but complications, especially pneumonia, can lead to serious illness or death.[3] A study estimated that 291243–645832 seasonal influenza associated respiratory deaths occur annually worldwide.[4] The mortality caused by severe influenza is more than three times that of community-acquired pneumonia.[5] Influenza virus is the most common pathogen causing viral pneumonia,[6] which is characterized by high levels of viral replication and strong pro-inflammatory response induced by influenza virus. The excessive inflammatory response can be referred to as cytokine storm. An unremitting release of pro-inflammatory cytokines and chemokines was observed in severe cases caused by influenza infection,[7] which can lead to diffuse alveolar injury, hyaline membrane formation, fibrin exudation, and epithelial–endothelial barrier damage.[8] Controlling influenza virus-induced cytokine storm has been considered a vital strategy for treating influenza.[9] Immunomodulatory therapy has been recommended to ameliorate immune damage induced by cytokine storm. Corticosteroids are the most widely used and effective anti-inflammatory therapy. Favorable benefits of corticosteroid therapy in patients with severe community-acquired pneumonia have been observed.[10] Corticosteroid therapy has been found to ameliorate acute lung injury (ALI) induced by influenza virus in mice.[11] However, side effects, such as secondary bacterial or fungal infection and prolonged viral shedding, have been observed in patients with influenza infection.[12,13] More effective agents are urgently required for treatment of the hyperinflammation status caused by influenza. Antiviral drugs are the primary treatment for influenza, but some agents are faced with drug resistance. Globally, more than 45% of influenza A virus subtypes are resistant to adamantanes as of 2013.[14] Neuraminidase inhibitors and baloxavir marboxil are also confronted with drug resistance.[15] Effective treatment strategies for influenza infection are urgently needed.

Traditional Chinese Medicines (TCMs) have been utilized for treatment of diseases characterized by fever, cough and rhinorrhea for thousands of years. Notably, TCMs have been recommended by the Chinese government for treatment of influenza infection in China for many years. Benefits of TCMs in treatment for influenza have been observed. Significant improvement in symptoms has been made by TCMs.[16] The mechanism of TCMs against influenza is versatile with characteristics of multitarget, multipathway and multisystem by regulating the immune response and alleviating the

inflammation through targeting the host signaling pathway.[17] Baicalin, a natural compound from TCMs, could modulate macrophage polarization, reduce macrophage recruitment in the lung and mitigate ALI caused by influenza virus.[18] Multiple active ingredients, such as ergosterol peroxide[19] and erucic acid[20] isolated from *Radix isatidis*, could suppress the inflammation induced by influenza via downregulating RIG-I and mitogen-activated protein kinase 14 (p38) MAPK signaling pathway. GeGen QinLian decoction, an effective agent for influenza infection, could significantly ameliorate ALI and suppress the pro-inflammatory response induced by influenza virus via blocking the TLR7 signaling pathway[21] and downregulating the NOD/RIP2/NF-κB signaling pathway in the intestine.[22]

BaBaoWuDanYaoMo (BB), a TCM, consists of 22 herbs including *Babalus bubalis* Linnaeus, *Saigae tataricae* Linnaeus, *Moschus*, Borneolum Syntheticum, the shell of *Pernulo*, the excretion of *Venenum Bufonis, Calculus Bovis Sativus*, Cinnabar, the gallbladder of *Bos taurus*, Fel Ursi, the gallbladder of *Zaocys dhumnades*, Pulvis Fellis Suis (the dried bile of *Sus scrofa domestica* Brisson), the gallbladder of *Mylopharyngodon piceus, Chuanxiong Rhizoma, Eugenia caryophyllata* Thunb, *Nelumbo nucifera* Gaertn, *Spica prunellae, Carthamus tinctorius* L., *Cirsium setosum* (Willd). MB., *Cirsium japonicum* DC., the roots of *Imperata cylindrica and Paeonia suffruticosa* Andr. *Cornu saigae tataricae* has been widely used in patients with high fever or influenza infection.[23] Liu Shen Wan, consisting of 6 TCMs including *Moschus*, Borneolum syntheticum, *Calculus Bovis Sativus*, the excretion of *Venenum Bufonis and* the shell of *Pernulo* from BB, poses antiviral and anti-inflammatory pharmacological activity against influenza[24] and has been used as treatment for influenza infection.[25] Multiple herbs of BB such as *Cirsium japonicum* DC., *Cirsium setosum* (Willd). MB., *Paeonia suffruticosa* Andr., *Eugenia caryophyllata* Thunb, *Imperata cylindrica* and *Spica prunellae* have the characteristics of antibacterial, antitumor and immunomodulatory effects. Some herbs of BB, including *Carthamus tinctorius* L.[26] and *Chuanxiong Rhizoma*,[27] inhibit the pro-inflammatory mediators (IL-6, TNF-α and IL-10) induced by lipopolysaccharide (LPS) via downregulating NF-κB signaling pathway. β-sitosterol,[28] an active ingredient of common Chinese medical plants, such as *Eugenia caryophyllata* Thunb, *Cirsium setosum* (Willd). MB., *Carthamus tinctorius* L. and *Spica prunellae*, has been found to alleviate influenza A virus-induced proinflammatory response and ALI. Antiviral drugs would be confronted with drug resistance for viral mutation on its targeted protein. BB may be a promising agent for inhibiting virus-induced inflammatory response by targeting multiple host protein, which may effectively address drug resistance challenges originating from viral mutation. However, the effect of BB against influenza virus remains obscure. In this study, we aim to predict the underlying mechanism of BB against influenza virus infection. The results confirmed the effect of BB in mice infected with influenza A virus and verified the mechanism of BB against the inflammatory response induced by influenza in vitro.

Material and Methods
Candidate Compound Screening and Identification of Drug Targets
The chemical ingredients of BB and its related targets were collected from database platforms (TCMSP and BATMAN-TCM).[29,30] The ingredients were retained for further analysis according to the criteria of oral bioavailability (OB) ≥30% and drug-likeness (DL) ≥0.18. Multiple disease-related databases (Genecard, Drugbank, DisGeNET and CTD) were used for collection of influenza-related targets.[29,30] These targets were utilized to obtain the potential targets of BB for the treatment of influenza via the Wayne diagram.[29,30]

Protein–Protein Interaction Data
The Protein–Protein interactions of these targets were built to find the core targets of BB for treatment of influenza infection. The targets for the treatment of influenza infections were collected via the Wayne diagram as described above. Influenza-related targets were obtained from the STRING tool[29,30] with the combine score greater than or equal to 0.9. All the species were limited to "Homo sapiens". The PPI relationship network was constructed through Cytoscape (ver.3.7.2).

Gene Ontology (GO) and Kyoto Encyclopedia of Genes and Genomes (KEGG) Pathway Enrichment Analysis of Targets

GO analysis and KEGG pathway enrichment analysis[29,30] were employed to predict the underlying biological processes and signaling pathways of BB for the treatment of influenza. Pathways with p values less than 0.05 were selected for further analysis.

Network Construction

The Cytoscape (ver.3.7.2) software was employed to construct the compound-target-disease (C-T-D) diagram using the targets from the influenza-related signaling pathway obtained through KEGG pathway enrichment analysis.

Molecular Docking

To determine the binding sites and binding activity of compounds with key targets, the core targets were docked with compounds via CB-Dock website (http://cao.labshare.cn/cb-dock/), which was highly consistent with AutoDock Vina and had been optimized with a success rate of 70%.[31] The respective and inflammation-related targets were obtained from PPI network and KEGG analysis. The compounds that targeted the core proteins above were obtained from the C-T-D diagram via Cytoscape (ver.3.7.2) software. The protein (PDB format) and three-dimensional (3D) structures of compound (.sdf file format) were acquired from PDB and PubChem database, respectively. The vina scores (kJ/mol) and cavity size were acquired on the CB-Dock website. The lowest value was displayed at the top and selected for evaluating their binding activity. The binding sites were visualized using PyMOL software.

Reagents

BB (lot: Z34020249) was provided by Anhui Moyao Pharmaceutical Co., Ltd. (Anhui, China). In in vitro experiments, the BB was dissolved in dimethyl sulfoxide (DMSO) to 100 mg/mL. Then, it was diluted to 1 mg/mL using DMEM/F12 (1:1) without fetal bovine serum (FBS) as a stock solution and stored at $-20°C$ prior to use. However, in in vivo experiments, BB was melted in phosphate-buffered saline (PBS) to three concentrations (500, 250, and 125 mg/kg). Oseltamivir phosphate (lot: 196618–13-0, Stru Chem Co., Ltd, China) provided by HEC Pharmaceutical Industry was dissolved in DMSO to 100 mm for in vitro experiments, but it was melted in PBS to 80 mg/kg for in vivo experiments. AKT (lot: 2965, CST, Shanghai, China), phosphorylated p38 (lot: 4511, CST, Shanghai, China), p38 (lot: 9212, CST, Shanghai, China), phosphorylated AKT (lot: 4060, CST, Shanghai, China), TLR3 (lot: 6961, CST, Shanghai, China), GAPDH (lot: 2118, CST, Shanghai, China), PARP (lot: 9532, CST, Shanghai, China) and Cleaved PARP (lot: 5625, CST, Shanghai, China) were purchased from Cell Signaling Technology.

Viruses and Cells

Madin-Darby canine kidney (MDCK) and the human lung carcinoma A549 cells were purchased from American Type Culture Collection (ATCC, USA) and cultured at 37°C in a humidified atmosphere of 5% CO_2 in DMEM/F12 (1:1) medium (Gibco, USA) with 10% FBS. The influenza A/PR/8/34 (H1N1) (PR8), Guangzhou/GIRD02/2009 (H1N1) (09H1N1), A/Aichi/2/68 (H3N2), and A/HK/Y280/97 (H9N2) were stored at $-80°C$. The viral titer was determined via a 50% tissue culture infective dose ($TCID_{50}$) assay and calculated by the Reed–Muench method prior to use. The $TCID_{50}$ of PR8, 09H1N1, H3N2 and H9N2 was $10^{-7.2}$, $10^{-5.5}$, $10^{-6.3}$, and $10^{-6.4}$, respectively.

Cytotoxicity Assay

The cytotoxic effect of BB on MDCK and A549 cells was determined using a 3-(4,5-dimethylthiazol-2-yl)-2,5-diphenyltetrazolium bromide (MTT) assay. In summary, the MDCK cells (2×10^4 cells/well) were seeded into 96-well plates for 24 h and subsequently rinsed with PBS. Then, the medium was replaced with different concentrations of BB. Subsequently, after being washed with PBS, the cells were stained with MTT solution (1 mg/mL) for 4 h. The formazan crystals generated in each well were dissolved with DMSO. The absorbance was determined at 490 nm using a microplate reader (Thermo Fisher, USA).

Protective Effects of BB

The protective effect of BB against virus-induced cell death including PR8, 09H1N1, H3N2 and H9N2 were evaluated on MDCK cells. Cells were cultured in 96-well plates for 24 h to monolayer, the original medium was discarded, and the cells were washed once with PBS. Cells were inoculated with 100 $TCID_{50}$ viruses for 2 h. After being washed by PBS, the cells were cultured in 96-well plates in the presence of different concentrations of BB cultured solution in DMEM/F12 containing 2 μg/mL TPCK trypsin (Sigma), followed by incubation at 37°C under 5% CO_2 for 48 h. The percentage of CPE was recorded, and the 50% inhibition concentration (IC_{50}) of the virus-induced CPE by BB was calculated. The selectivity index (SI) was determined by the TC_{50}/IC_{50} ratio.

Mitochondrial Membrane Potentials Assay

Mitochondrial transmembrane potential ($\Delta\Psi m$) was determined with the mitochondrial membrane potential assay kit with JC-1 (Beyotime, Shanghai, China). A549 cells were infected with PR8 at 1 MOI for 2 h in 12-well plates. After 2 h incubation, cells were incubated with indicated concentrations of BB for 24 h. Subsequently, the cells were incubated at 37°C for 20 min with 0.5 mL of JC-1 working solution. Then, the staining solution was removed, and the cells were washed twice with JC-1 staining 1 × buffer. Finally, $\Delta\Psi m$ was observed by fluorescence microscopy at 100× (Leica Micro-systems CMS GmbH inverted fluorescence microscope). Green fluorescence represented a decrease in mitochondrial membrane potential, indicating that the cell was likely to be in the early stage of apoptosis. Cell treated with 10 μM carbonyl cyanide m-chlorophenylhydrazone (CCCP) was used as negative control. CCCP was a protonophore that could cause dissipation of $\Delta\Psi m$.

Quantitative Real-Time PCR Assay

A549 cells were inoculated in six-well cell plates and cultured at 37°C under 5% CO_2 for 24 h until more than 90% fused. The original medium was discarded, and the cells were washed once with PBS. After being inoculated with virus (MOI = 0.5) for 2 h at 37°C, the inoculum was replaced with the indicated concentrations of BB or mock-treated with DMEM/F12 for subsequent 24 h incubation. After 24 h of drug treatment, total RNA was extracted according to the specification of RNA reagent (Invitrogen, MA, USA). Reverse transcription of RNAs was quantified using the PrimeScript™ RT Master Mix kit (Takara Bio, Japan). RT-PCR was performed on cDNA samples by Tag Man Premix Ex Tap TM II (Takara Bio, Japan). The PCR data were analyzed using the detection system (ABI PRISM® 7500 Real-time PCR system, Applied Biosystems Co., USA). The relative amount of PCR products was calculated using the $2^{-\Delta\Delta Ct}$ method as previously described. Primers for interleukin-6 (IL-6), interleukin-8 (CXCL-8/IL-8), C-X-C motif chemokine 10 (CXCL-10/IP-10), tumor necrosis factor-α (TNF-α), and C-C motif chemokine 2 (MCP-1/CCL-2) genes (Table 1) were designed using primer 5.0.

Table 1 Primer Sequence for RT-qPCR for 6 Targeted Genes

Target Gene	Direction	Sequence (5′-3′)
IL-6	Forward	CGGGAACGAAAGAGAAGCTCTA
	Reverse	CGCTTGTGGAGAAGGAGTTCA
CXCL-2/MIP-2	Forward	TTGGCAGCCTTCCTGATTTC
	Reverse	TATGCACTGACATCTAAGTTCTTTAGCA
CXCL-10/IP-10	Forward	GAAATTATTCCTGCAAGCCAATTT
	Reverse	TCACCCTTCTTTTTCAT-TGTAGCA
TNF-α	Forward	AACATCCAACCTTCCCAAACG
	Reverse	GACCCTAAGCCCCCAATTCTC
MCP-1/CCL-2	Forward	CAAGCAGAAGTGGGTTCAGGAT
	Reverse	AGTGAGTGTTCAAGTCTTCGGAGTT
GAPDH	Forward	GAAGGTGAAGGTCGGAGTC
	Reverse	GAAGATGGTGATGGGATTTC

Western Blot Assay

After pre-cooling the cells in PBS, the cells were lysed with RIPA lysis buffer (DGCS Biotechnology, China) containing a protease inhibitor cocktail (Sigma-Aldrich). The protein concentrations of the cell samples were measured by the BCA kit (Beyotime, China). Denatured protein samples (25 μg) were subjected to 10% SDS-PAGE gel electrophoresis. The proteins were transferred to PVDF membranes using a BIO-RAD transmembrane instrument. Then, the PVDF membranes were sealed with 5% BSA for 1 h. After being incubated overnight at 4°C, the PVDF membranes were washed with TBST on the next day, and the corresponding HRP-labeled antibodies were incubated at room temperature.

Antiviral and Anti-Inflammatory Assay in vivo

Specific pathogen-free female BALB/c mice (20–22 g, 5 to 6 weeks old, Certificate No. GZL0008) were obtained from Hunan SJA Laboratory Animal Co. Ltd (Hunan, China). The mice were housed in the cage at 22 ± 1°C with a relative humidity of 50 ± 10% and a 12-h light/dark cycle. The experiments related to animals were conducted in accordance with the guidelines of the Ethics Committee of Guangzhou Medical University for the management of experimental animals and were approved by the Ethics Committee of Guangzhou Medical University (2021061). All animals were anaesthetized with propofol and euthanized. In the course of animal experiments, efforts were made to minimize animal suffering.

A total of 60 BALB/c mice were randomly allocated into 6 groups with per group of 10 mice including normal group, model group, oseltamivir group (80 mg/kg), and BB group (500, 250, and 125 mg/kg). The BALB/c mice were anesthetized and inoculated intranasally with 50 μL viral suspension containing 1 LD_{50} (50% lethal dose) of PR8 in the infected group or PBS in the normal control group (NC) to determine the anti-inflammatory effects of BB on mice infected with influenza virus. After being infected for 2 h, the infected mice were orally administrated BB (500, 250, and 125 mg/kg/day), oseltamivir (80 mg/kg/day), or PBS daily for five days. On day 6 after infection, the mice were anesthetized and euthanized. The whole lungs were harvested and weighed to calculate the lung index (lung index = lung weight/body weight). The left lung lobes were fixed in 4% formaldehyde for histopathological examination. The right lung lobes were homogenized and stored at −80°C. The mRNA expression of cytokines in the lungs was determined by real-time fluorescence quantitative PCR. Primers for C-X-C motif chemokine 9 (CXCL9/MIG), TNF-α, C-X-C motif chemokine 1 (CXCL1/KC) and interleukin-1 beta (IL-1β) were designed using Primer 5.0 (Table 2).

Table 2 Primer Sequence for RT-qPCR for 5 Targeted Genes

Target Gene	Direction	Sequence (5′-3′)
CXCL9/MIG	Forward	GAACCCTAGTGATAAGGAATGCA
	Reverse	CTGTTTGAGGTCTTTGAGGGATT
	Probe	5'FAM-CATCAGCACCAGCCGAGGCACG-3'BHQ1
TNF-α	Forward	CATCTTCTCAAAATTCGAGTGACAA
	Reverse	TGGGAGTAGACAAGGTACAACCC
	Probe	5'FAM-CACGTCGTAGCAAACCACCAAGTGGA-3'TAMRA
CXCL1/KC	Forward	GGCGCCTATCGCCAATG
	Reverse	CTGGATGTTCTTGAGGTGAATCC
	Probe	5'FAM-CGCTGTCAGTGCCTGCAGACCATG-3'TAMRA
IL-1β	Forward	AACCTGCTGGTGTGTGACGTTC
	Reverse	CAGCACGAGGCTTTTTTGTTGT
	Probe	5'FAM-TTAGACAGCTGCACTACAGGCTCCGAGATG-3'TAMRA
GADPH	Forward	CAACTACATGGTCTACATGTTC
	Reverse	CTCGCTCCTGGAAGATG
	Probe	5'FAM-AGTCCCACTCAGACCCAGCAGG-3'BHQ1

Statistical Analysis

All the data in this study were analyzed using the analysis of variance (ANOVA) with SPSS ver. 25.0 (Armonk, NY, USA). Data were presented as mean ± standard deviation (S.D). The differences in the different groups were detected by the one-way ANOVA analysis. P-value <0.05 was considered statistically significant.

Results

Compound Information and Key Targets for BB Against Influenza

BB comprises 22 Chinese medicines. A total of 182 active compounds were obtained based on the criteria of oral bioavailability (OB) ≥30% and drug-likeness (DL) ≥0.18, and 934 influenza targets were obtained. In addition, 1917 BB-related targets were obtained from BATMAN and TCMSP databases on the basis of 182 active compounds. A total of 155 ingredients participated in influenza infection, and 192 overlapping targets were employed to construct the PPI network (Figure 1A and B). The PPI relationship network has 128 nodes and 574 edges. Analyzing the topological parameters of PPI relationship network assists in identifying the core targets. The larger node indicates higher degree and more important network. According to the criterion of degree >20, 14 key target genes involved in influenza infection were determined, as shown in Table 3.

GO and KEGG Enrichment Analysis for Potential Mechanism Against Influenza Infection

A total of 192 candidate targets were analyzed by GO enrichment analysis and KEGG enrichment to predict the mechanism of BB against influenza infection. A total of 710 biological processes were obtained by GO analysis, from which the top 20 terms were selected ($p < 0.05$) (Figure 2). The top 10 biological processes were positive regulation of transcription from RNA polymerase II promoter, signal transduction, inflammatory response, positive regulation of transcription DNA-templated, negative regulation of apoptotic process, positive regulation of gene expression, response to drug, apoptotic process, immune response and positive regulation of cell proliferation. Influenza-induced inflammation could contribute to disease severity, leading to high morbidity and mortality rates. Regulating the inflammatory response induced by influenza had been considered one of the key strategies for influenza infection, especially for the severe cases.
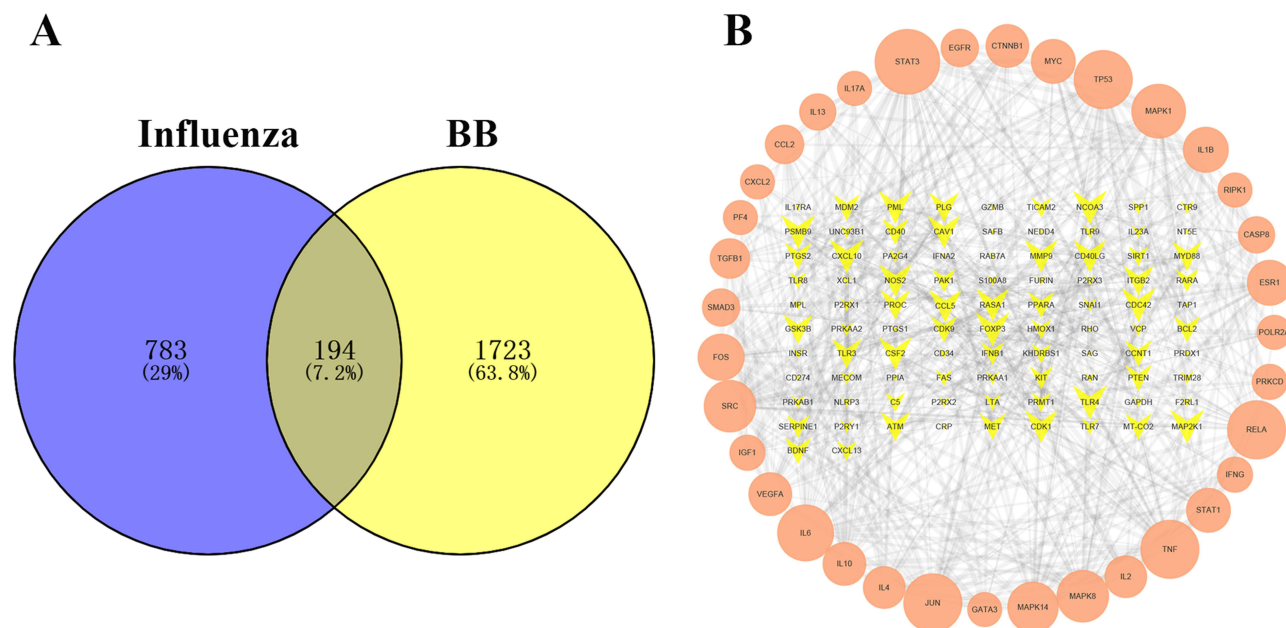

Figure 1 Influenza infection-related targets by BB. (**A**) The Venn diagram of targets between 182 active compounds-related targets and targets of influenza A viral infection. The purple circular shape represented 934 influenza-related targets. The yellow circular shape represented 1725 active ingredients. The overlapping shape represented 192 influenza-related targets by BB. (**B**) The Protein–Protein interactions of 192 targets. The size of a node was directly consistent with its degree. The degree of Orange nodes is over 11, while the degree of yellow nodes is below 11.

Table 3 The Top 14 BB-Related Targets (Degree > 20) Involved in Influenza Infection

UniProt ID	Protein Name	Gene Name	Degree
P40763	Signal transducer and activator of transcription 3	STAT3	39
P05412	Transcription factor AP-1	JUN	33
P01375	Tumor necrosis factor	TNF	33
Q04206	Transcription factor p65	RELA	33
P04637	Cellular tumor antigen p53	TP53	33
P05231	Interleukin-6	IL6	31
P28482	Mitogen-activated protein kinase 1	MAPK1	29
P12931	Proto-oncogene tyrosine-protein kinase Src	SRC	27
P45983	Mitogen-activated protein kinase 8	MAPK8	27
Q16539	Mitogen-activated protein kinase 14	MAPK14	26
P01100	Proto-oncogene c-Fos	FOS	22
P01584	Interleukin-1 beta	IL1β	21
P03372	Estrogen receptor	ESR1	21
P42224	Signal transducer and activator of transcription 1-alpha/beta	STAT1	20

Negative regulation of apoptotic process was also a strategy to intervene in the proliferation of influenza virus. Most importantly, regulating the inflammatory response and negative regulation of apoptotic process may be the key biological processes for BB to intervene influenza infection.
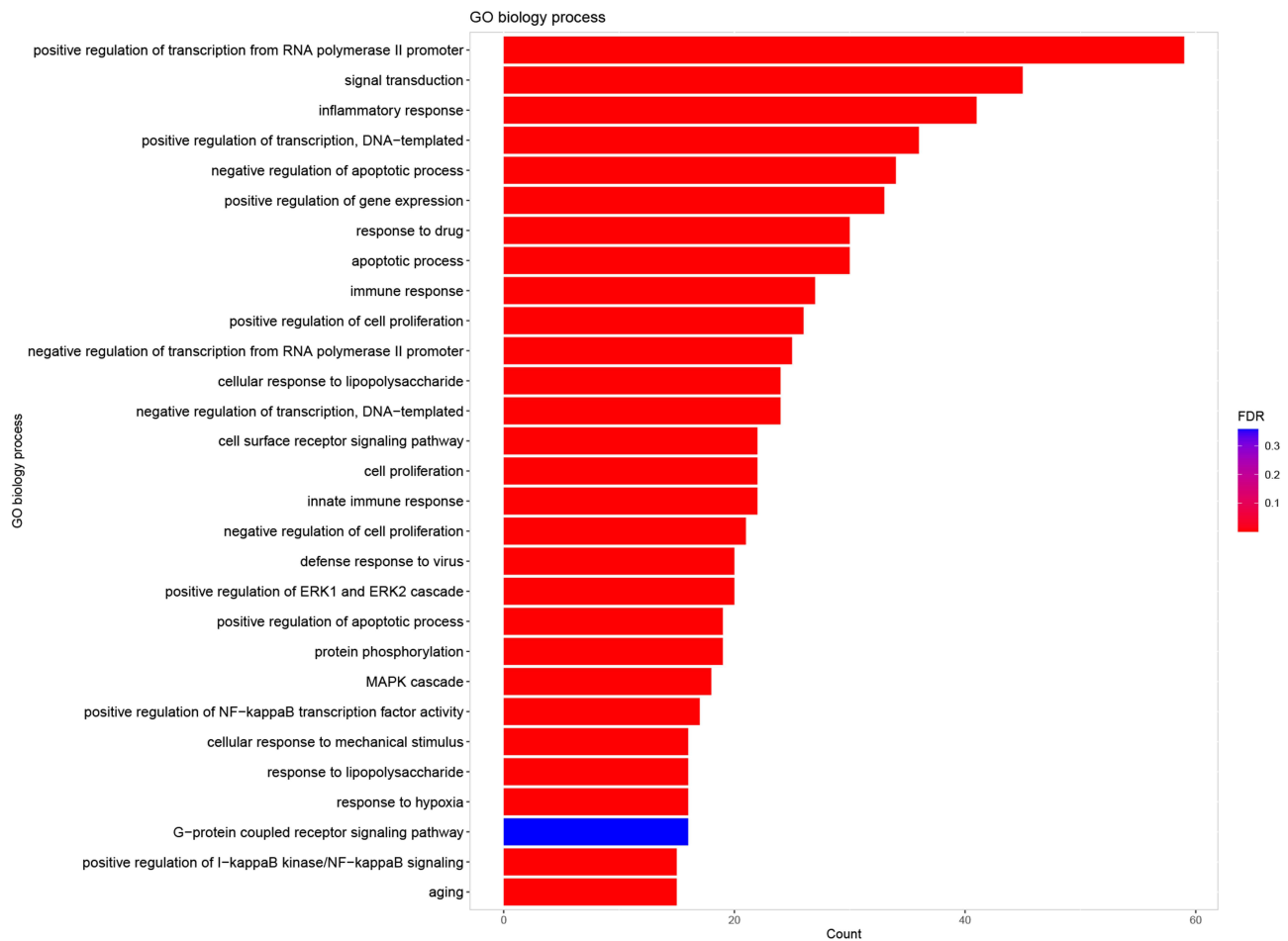

Figure 2 Top 20 biological processes of BB. X-axis showed ratio and Y-axis showed involved terms. Count and *p*-values were shown on right.

A total of 106 signaling pathways were obtained from KEGG analysis, from which the top 20 terms were selected as well ($p < 0.05$) (Figure 3A). Among the top 20 signaling pathways, influenza A, toll-like receptor signaling pathway, MAPK signaling pathway and phosphatidylinositol 3-kinase-serine/threonine kinase (PI3K-AKT) signaling pathway were vital signaling pathways involved in influenza infection, especially influenza-induced inflammation (Figure 3B). These results supported the hypothesis that BB alleviated the severity of influenza infection, at least in part through blocking these signaling pathways to regulate inflammatory response. The key targets of these signaling pathways are shown in Figure 3B.

Network Construction

To expound the multicomponent and multitarget mechanism of BB in the treatment of influenza, the C-T-D networks were constructed using Cytoscape (ver.3.7.2). The information of target genes such as gene ID and organism were acquired using the UniProt database. The C-T-D network consisted of 96 nodes and 107 edges (Figure 4). The larger
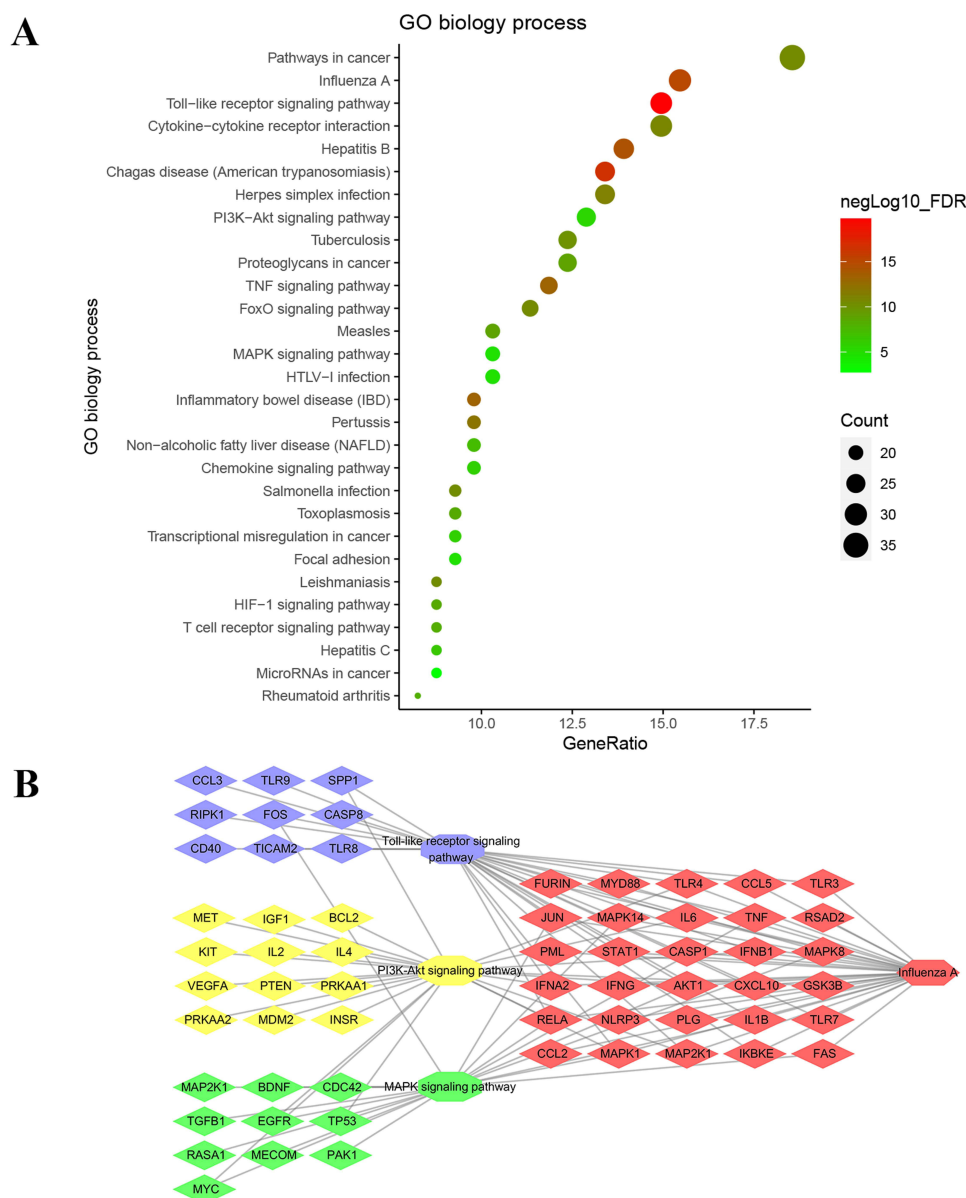

Figure 3 Top 20 KEGG pathways and key protein targets. (**A**) Top 20 KEGG pathways of BB. X-axis showed ratio and Y-axis showed involved terms. Count and *p*-values were shown on right. (**B**) Critical targets of influenza A, toll like receptor signaling pathway, MAPK signaling pathway and PI3K- AKT signaling pathway involved in influenza infection by BB.

Figure 4 BB component-target-disease network. Purple diamond nodes represented the disease nodes, red diamond nodes represented the targets, yellow diamond nodes represented Chinese medicines and green nodes represented active ingredients.

degree indicates a more important compound. As shown in Table 4, quercetin, kaempferol, β-sitosterol, testosterone, methoxybufotenin, and 17-β-estradiol were part of core compounds with larger degrees. Among these core components, β-sitosterol,[19] quercetin,[32] and kaempferol[33] have been found to have antiviral and anti-inflammatory activities against influenza.

Table 4 The Critical Compounds of BB Involved in Influenza Infection

Molecule Name	MOL ID	MW	OB (%)	DL	Degree
Quercetin	MOL000098	302.25	46.43	0.28	16
Kaempferol	MOL000422	286.25	41.88	0.24	10
Beta-sitosterol	MOL000358	414.79	36.91	0.75	9
Testosterone	MOL001232	288.47	12.93	0.35	7
Methoxybufotenin	MOL004024	218.33	63.78	0.09	7
17-Beta-Estradiol	MOL010919	272.42	12.41	0.32	6
Cholesterol	MOL000987	384.76	5.69	0.67	5
Alanine	MOL000042	89.11	87.69	0.01	5
3-[2-[[3-(2-carboxyethyl)-4-methyl-5-[(E)-(4-methyl-5-oxo-3-vinyl-2-pyrrolylidene) methyl]-1H-pyrrol-2-yl] methyl]-4-methyl-5-[(Z)-(3-methyl-5-oxo-4-vinyl-2-pyrrolylidene) methyl]-1H-pyrrol-3-yl] propanoic acid	MOL008835	584.73	16.53	0.75	5
3,5-Dihydroxybenzoic Acid	/	154.12	/	/	5
Decamine	/	221.04	/	/	4
Bufothionine	/	267.33	/	/	4
Androst-4-Ene-3,17-Dione	/	286.41	/	/	4
γ-aminobutyric acid	/	120.15	/	/	3
SPBio_002209	MOL002014	204.39	28.21	0.06	3
p-Ocimene	MOL000201	136.26	15.06	0.02	3
Myrcene	MOL000197	136.26	24.96	0.02	3
Hemo-sol	MOL000023	136.26	39.84	0.02	3
Guanidine	MOL006394	59.09	24.00	0.00	3
Deoxycholicacid	MOL008845	392.64	40.72	0.68	3
D-Camphene	MOL000019	136.26	34.98	0.04	3

(*Continued*)

Table 4 (Continued).

Molecule Name	MOL ID	MW	OB (%)	DL	Degree
CHEBI:7	MOL000270	136.26	45.20	0.04	3
Campesterol	MOL005438	400.76	37.58	0.71	3
Beta-Humulene	MOL000029	204.39	26.87	0.06	3
Beta-caryophyllene	MOL000036	204.39	29.70	0.09	3
Alpha-pinenepinene	MOL006867	124.25	47.43	0.02	3
Allantoin	MOL002347	158.14	96.90	0.03	3
(S)-(+)-alpha-Phellandrene	MOL000200	136.26	27.90	0.02	3
()-beta-Pinene	MOL000905	136.26	44.77	0.05	3
Ursodeoxycholic Acid	/	/	/	/	2
Tauroursodeoxycholic Acid	/	/	/	/	2
Myricanone	MOL002135	356.45	40.60	0.51	2
Methyl desoxycholate	MOL008839	406.67	34.63	0.73	2
Hyoscine	MOL011519	303.39	49.84	0.27	2
fa	MOL000433	441.45	68.96	0.71	2
Estragole	MOL002361	148.22	36.59	0.03	2
Ergosterol	MOL000298	396.72	14.29	0.72	2
Elemicin	MOL000269	208.28	21.94	0.06	2
CLR	MOL000953	386.73	37.87	0.68	2
Cholicacid	MOL009807	408.64	22.17	0.72	2
Chenodeoxycholic acid	MOL008842	392.64	27.17	0.69	2
Bilicerdin	MOL008834	582.71	23.79	0.75	2
Beta-elemene	MOL000908	204.39	25.63	0.06	2
Androsterone	/	290.44	/	/	2
Alpha-Hyodeoxycholic Acid	/	392.6	/	/	2
5-Cis-Cyclotetradecen-1-One	/	/	/	/	2
5-Cis-Cyclopentadecen-1-One	/	/	/	/	2
3-beta-Hydroxy-5alpha-Androstan-17-One	/	290.40	/	/	2
3alpha-Hydroxy-5alpha-Androstan-17-One	/	290.4	/	/	2
Beta-Hyodeoxycholic	/	392.6	/	/	2
Beta-elemene	/	204.35	/	/	2

Compound-Target Docking

Molecular docking was employed to analyze the structural complexes of the targets to explore the binding activities of core compounds with targets. The top Vina scores and cavity size were obtained from CB-Dock website. In general, the value of Vina scores reflected a certain binding activity between a protein and a compound. The more negative Vina score indicates that a more stable compound binds to the target. In addition, the accuracy tends to increase when the cavity size is close to even larger than the ligand.[31] Our results indicated that multiple ingredients bound well with transcription factor p65 (RELA), Mitogen-activated protein kinase 1 (MAPK1), Toll-like receptor 3 (TLR3), Toll-like receptor 7 (TLR7) and AKT1 (Table 5). Quercetin, testosterone, bufothionine, decamine and campesterol had the strongest binding activity with RELA (Figure 5A), MAPK1 (Figure 5B), TLR3 (Figure 5C), TLR7 (Figure 5D) and AKT1 (Figure 5E), respectively. Their binding sites were shown in Figure 5.

Protective Effect of BB

The protective effect in MDCK cells of BB on different subtypes of influenza virus strains including human influenza viruses (H1N1 and H3N2) and avian influenza viruses (H9N2) was tested by CPE assays to investigate the anti-influenza activities of BB. The median toxic concentration (TC_{50}) of BB in alveolar epithelial (A549) (Figure 6A) and MDCK (Figure 6B) cells was 221.4 and 236.5 μg/mL, respectively. The 50% inhibitory concentration (IC_{50}) of BB against influenza A virus strains, including PR8, 09H1N1, H9N2, and H3N2, were 116.5 ± 2.2,

Table 5 The Top Vina Scores and Cavities Size of the Compounds with the Targets

Gene	PDB ID	Chemical Name	InChI Key	Vina Scores (kJ/mol)	Cavity Size
RELA	6ypl	17-Beta-Estradiol	VOXZDWNPVJITMN-ZBRFXRBCSA-N	−6.5	361
		Testosterone	MUMGGOZAMZWBJJ-DYKIIFRCSA-N	−7.3	361
		Kaempferol	IYRMWMYZSQPJKC-UHFFFAOYSA-N	−7.2	361
		Quercetin	REFJWTPEDVJJIY-UHFFFAOYSA-N	−7.3	361
MAPK1	6g92	17-Beta-Estradiol	VOXZDWNPVJITMN-ZBRFXRBCSA-N	−7.9	160
		Testosterone	MUMGGOZAMZWBJJ-DYKIIFRCSA-N	−8.0	654
		Quercetin	REFJWTPEDVJJIY-UHFFFAOYSA-N	−7.6	654
MAPK8	3o2m	Kaempferol	IYRMWMYZSQPJKC-UHFFFAOYSA-N	−7.9	921
MAPK14	1w7h	17-Beta-Estradiol	VOXZDWNPVJITMN-ZBRFXRBCSA-N	−8.7	404
STAT1	3wwt	Kaempferol	IYRMWMYZSQPJKC-UHFFFAOYSA-N	−6.9	921
		Quercetin	REFJWTPEDVJJIY-UHFFFAOYSA-N	−7.2	921
TLR3	2a0z	Bufothionine	XFIMEMVNMWDPRW-UHFFFAOYSA-O	−6.3	199
		Decamine	IHLKQCODTQXANL-UHFFFAOYSA-O	−6.0	162
TLR7	7cyn	Bufothionine	XFIMEMVNMWDPRW-UHFFFAOYSA-O	−6.3	276
		Decamine	IHLKQCODTQXANL-UHFFFAOYSA-O	−9.2	941
AKT1	4ekl	Methoxybufotenin	MOL008835	−6.4	1021
		Campesterol	SGNBVLSWZMBQTH-XAUDYDIZSA-N	−8.2	134
		Beta-sitosterol	PRLRGBPWIXOTPG-UIJMBHLFSA-N	−8.1	1021
		17-Beta-Estradiol	VOXZDWNPVJITMN-ZBRFXRBCSA-N	−7.1	1021
		Testosterone	MUMGGOZAMZWBJJ-DYKIIFRCSA-N	−7.9	130
		Kaempferol	IYRMWMYZSQPJKC-UHFFFAOYSA-N	−7.8	1021
		Quercetin	REFJWTPEDVJJIY-UHFFFAOYSA-N	−7.8	1021

59.86 ± 8.33, 66.43 ± 6.785, and 102.87 ± 6.66 μg/mL, respectively (Figure 6C–F). BB could efficiently reduce the CPE caused by virus in MDCK cells (Table 6). These results indicated that BB could protect cells from virus-induced cell death.

BB Decreases PR8-Induced Apoptosis in A549 Cells

GO and KEGG enrichment analysis inferred that the apoptotic process induced by influenza virus could be inhibited by BB. Mitochondrial membrane potential assays were carried out to reveal the underlying mechanism of BB against influenza infection, and the expression of cleaved PARP was determined to access the effect of BB on apoptotic process induced by PR8. Compared with the normal control group, the expression of cleaved PARP was significantly elevated. The expression of cleaved PARP was significantly inhibited by BB (125, 62.5, and 31.25 μg/mL) and oseltamivir (20 μM) ($p < 0.001$) (Figure 7A). Compared with the normal control group, a significant increase in apoptosis was induced by PR8. A significant decrease in apoptosis was observed in the BB group (125, 62.5, and 31.25 μg/mL) ($p < 0.001$ or $p < 0.01$) (Figure 7B–E). These results indicated that BB could suppress the apoptotic process caused by influenza virus.

BB Can Effectively Inhibit PR8-Induced Cytokines Expression in A549 Cells

According to the PPI network (Figure 1B and Table 3), IL-6, TNF-α, MCP-1/CCL-2, and CXCL-10/IP-10 were the most relevant inflammatory cytokines that BB may be involved in influenza infection. The mRNA expression of PR8-induced cytokines in A549 cells was detected by RT-qPCR to determine the inhibitory effect of BB on the inflammatory cytokines induced by PR8. As shown in Figure 8, the mRNA expression levels of MCP-1/CCL-2, IL-6, CXCL-8/IL-8, TNF-α, and CXCL-10/IP-10 were significantly upregulated in the model group compared with the normal control group ($p < 0.001$). Compared with the model group, BB (125, 62.5, and 31.25 μg/mL) could significantly inhibit the mRNA expression levels of MCP-1/CCL-2 (Figure 8A), IL-6 (Figure 8C), and CXCL-10/IP-10 (Figure 8D) ($p < 0.001$ or $p < 0.05$). In addition, compared with the model group, BB (125 and 62.5 μg/mL) could significantly suppress the mRNA expression of the CXCL/IL-8 (Figure 8E) ($p < 0.01$ or $p < 0.05$), and BB (125 μg/mL) could significantly decrease the mRNA expression of TNF-α
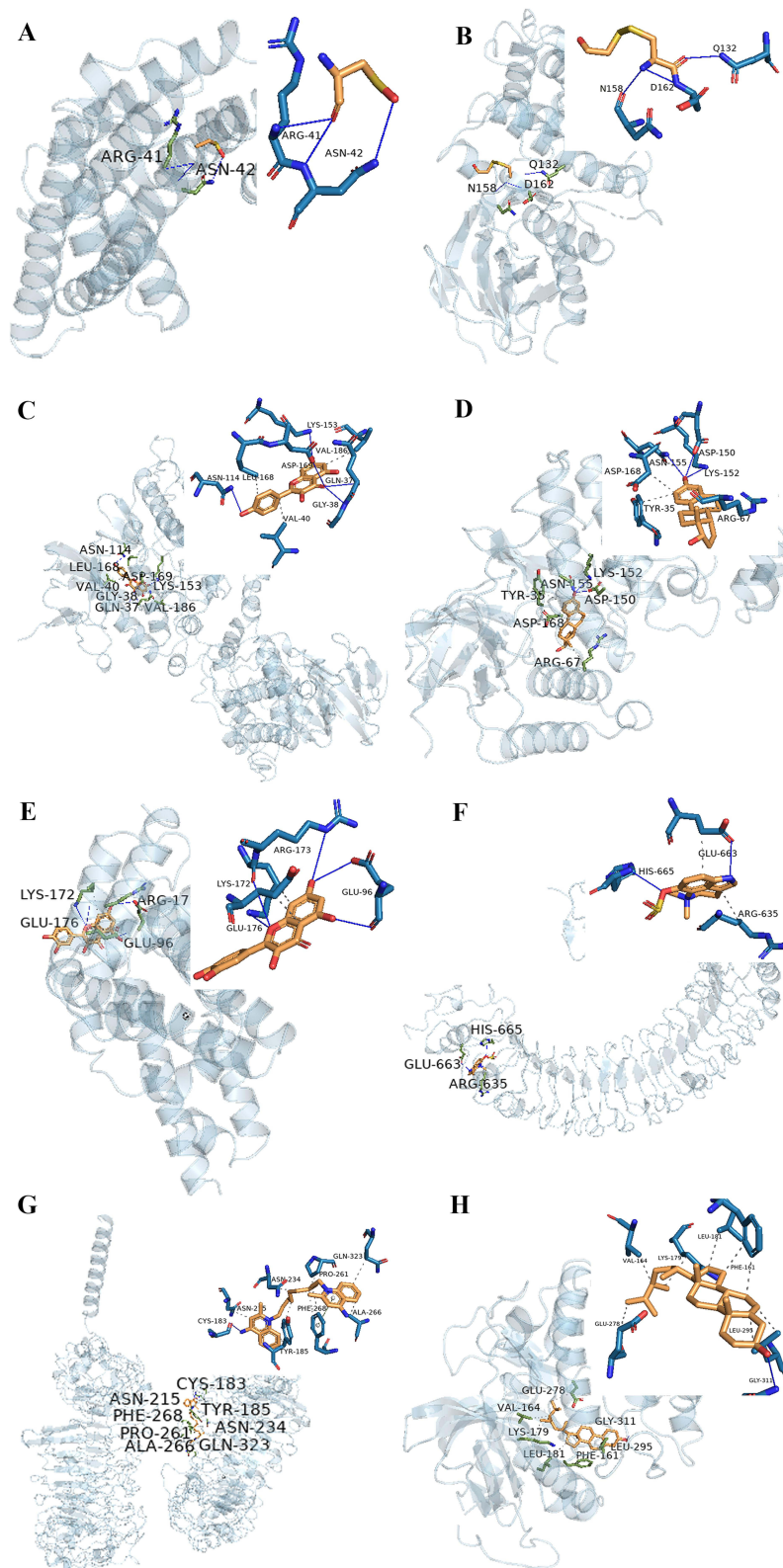
Figure 5 The ligand–receptor interaction of compounds and key targets. The overall structures of proteins (grey) in complex with compounds (golden). The localized interaction of compounds (blue) and proteins (golden) was shown on the right. (**A**) The localized interaction of quercetin with RELA; (**B**) testosterone with MAPK1; (**C**) kaempferol with MAPK8; (**D**) 17-Beta-Estradiol with MAPK14; (**E**) quercetin with STAT1; (**F**) bufothionine with TLR3; (**G**) decamine with TLR7; (**H**) campesterol with AKT1.
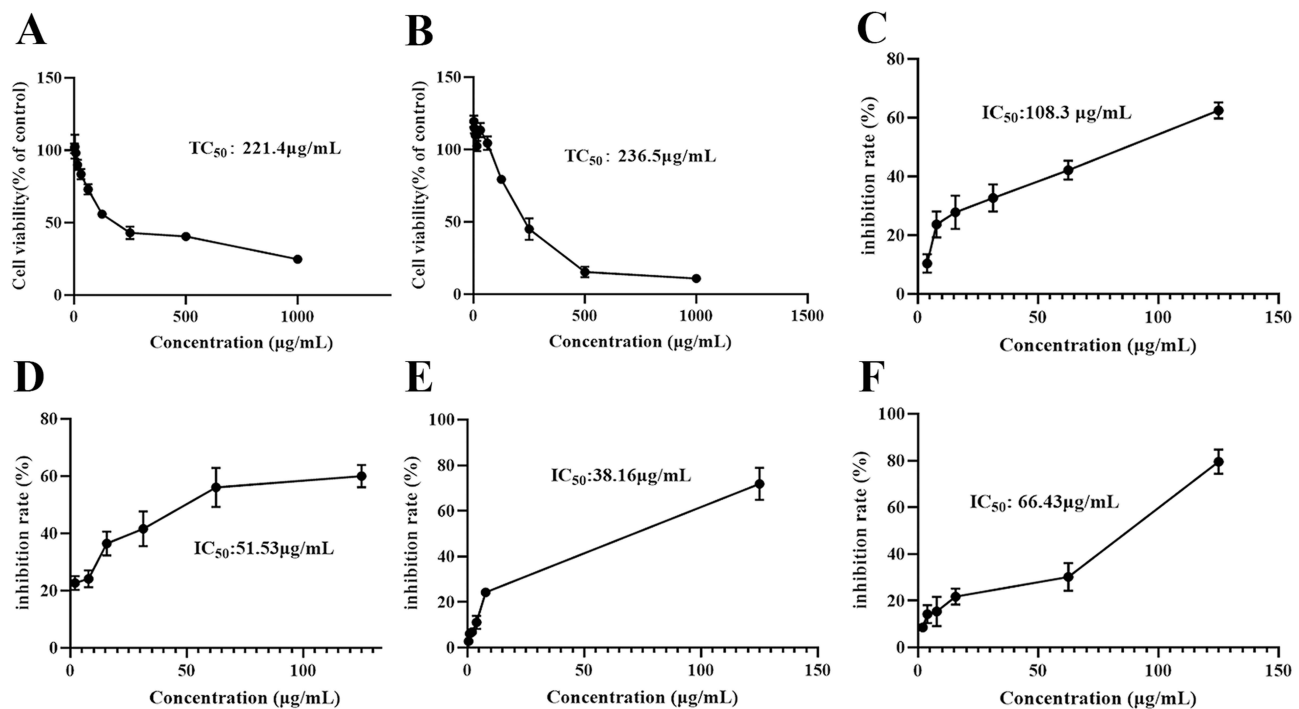
Figure 6 The protective effect of BB against influenza virus. (**A** and **B**) Cytotoxic effect of the BB on A549 cells and MDCK cells; (**C–F**) The protective effect of BB on different influenza A strains in MDCK cells, Error bars indicated the range of values obtained from counting in triplicate were represented as the mean ± SD of three individual experiments.

(Figure 8B) ($p < 0.05$). Compared with the model group, oseltamivir (20 μM) could also significantly inhibit the mRNA expression of the CXCL-8/IL-8, MCP-1/CCL-2 and IL-6 ($p < 0.001$). To our surprise, the inhibition effect of BB (125, 62.5, and 31.25 μg/mL) on IL-6 and CXCL-10/IP-10 was superior to oseltamivir (20 μM). However, the inhibition effect of BB (125 μg/mL) on MCP-1/CCL-2, TNF-α, and CXCL-8/IL-8 was better than oseltamivir (20 μM). These findings indicated that BB could inhibit the excessive release of pro-inflammatory mediators induced by PR8.

BB Can Inhibit the Phosphorylation of AKT/p38 Protein and TLR3 Protein Induced by PR8 in A549 Cells

According to the KEGG pathways analysis (Figure 4A) and PPI network (Figure 1B), TLR, MAPK, and PI3K-AKT signaling pathways were the key signaling pathways that BB might be involved in the inflammatory response. As shown in PPI network

Table 6 Anti-Influenza Virus Activities of BB in vitro

Influenza Subtype	IC$_{50}$ (μg/mL)	TC$_{50}$ (μg/mL)	SI
A/Puerto Rico/8/1934 (H1N1)	116.5±2.2	>236	>2.03
A/GZ/GIRD07/09 (H1N1)	59.86±8.33	>236	>3.94
A/HK/Y280/97 (H9N2)	66.43±6.785	>236	>3.55
A/Aichi/68 (H3N2)	102.87 ±6.66	>236	>2.29

Abbreviations: BB, BaBaoWuDanYaoMo; TCM, traditional Chinese medicine; PR8, A/PR/ 8 /34 (H1N1); GO, Gene Ontology; KEGG, Kyoto Encyclopedia of Genes and Genomes; OB, oral bioavailability; DL, drug-likeness; DAVID, database Visualization and Integrated Discovery system; MDCK, madin–Darby canine kidney; IL-6, interleukin-6; CXCL-8/IL-8, interleukin-8; CXCL-10/IP-10, C-X-C motif chemokine 10; TNF-α, Tumor necrosis factor-α; MCP-1/CCL-2, C-C motif chemokine 2; CXCL9/MIG, C-X-C motif chemokine 9; CXCL1/ KC, growth-regulated alpha protein; IL-1β, interleukin-1beta; A549, alveolar epithelial; CC50, 50% cytotoxic concentration; TC50, the median toxic concentration; TCID50, 100 × 50% tissue culture infective dose; FBS, foetal bovine serum; PBS, phosphate-buffered saline; CPE, cytopathic effect; RT-PCR, real-time polymerase chain reaction; 50% lethal dose, LD50; TLR3, toll-like receptor 3; ALI, acute lung injury.
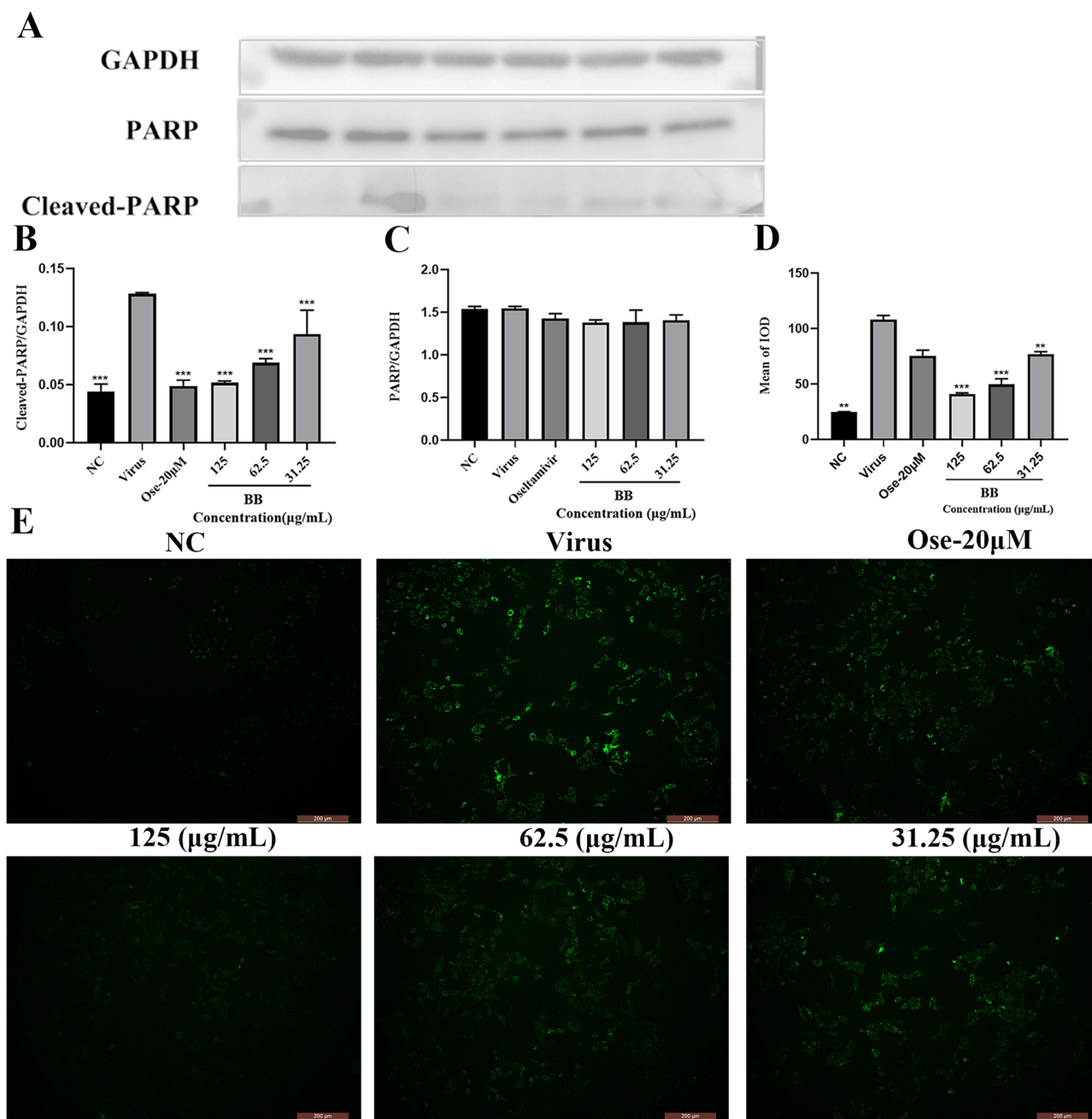
Figure 7 The effect of BB (125 μg/mL, 62.5 μg/mL and 31.25 μg/mL) or oseltamivir (20 μM) on the apoptotic process induced by PR8. (**A**) The inhibitory effect of BB on the expression of cleaved PARP; (**B** and **C**) The quantitative analysis of the cleaved PARP and PARP was analyzed by Image J; (**D**) The quantitative analysis of the apoptotic process induced by PR8; (**E**) A549 cells were stained by JC-1 and the change of ΔΨm was detected by fluorescence microscopy. *$p<0.05$; **$p<0.01$; ***$p<0.001$, when compared to the model group.

(Figure 1B), TLR3, MAPK14 and AKT were the key genes of TLR3, MAPK, and PI3K-AKT signaling pathways, respectively, related to influenza infection. p38 is encoded by MAPK14. We determined the effect of BB on TLR3, MAPK, and PI3K-AKT signaling pathways via the Western blotting assay to explore the underlying anti-inflammation mechanisms of BB. The phosphorylation of Akt/p38 protein and the protein expression of TLR3, p38, and AKT were determined (Figure 9A). Compared with the normal control group, a significant increase in the expression levels of TLR3 and the phosphorylation of AKT/p38 protein was induced in the model group. BB-treatment (125, 62.5, and 31.25 μg/mL) could significantly reduce the expression levels of TLR3 (Figure 9B) and the phosphorylation of p38 protein (Figure 9D) ($p < 0.001$ or $p < 0.01$ or $p < 0.05$). Compared with the model group, BB (125 μg/mL) could significantly decrease the phosphorylation of AKT protein (Figure 9E).
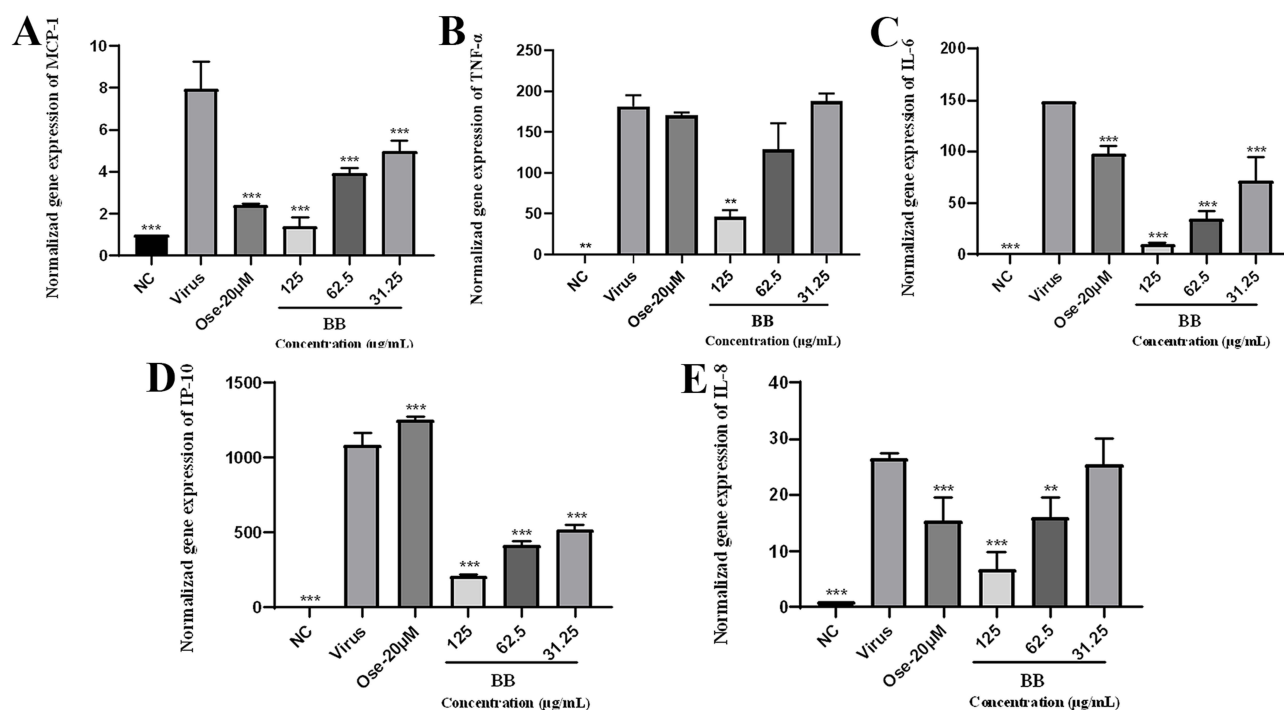
Figure 8 Effects of BB (125 μg/mL, 62.5 μg/mL and 31.25 μg/mL) or oseltamivir (20 μM) on the mRNA expression levels of pro-inflammatory mediators (MCP-1/CCL-2, IL-6, CXCL-8/IL-8, TNF-α, CXCL-10/IP-10) induced by PR8 in A549 cells. (**A**) The mRNA expression of the IL-6 in A549 cells; (**B**) The mRNA expression of the CXCL-8/IL-8 in A549 cells; (**C**) The mRNA expression of the CXCL-10/IP-10 in A549 cells; (**D**) The mRNA expression of the MCP-1/CCL-2 in A549 cells; (**E**) The mRNA expression of the TNF-α in A549 cells. The values were presented as the means ± S.D. of three individual experiments. *$p<0.05$; **$p<0.01$; ***$p<0.001$, when compared to the model group.

However, oseltamivir (20 μM) only inhibited the phosphorylation of p38 protein (Figure 9D). In addition, the expression of p38 MAPK and AKT had no significant difference (Figure 9C and F). These results inferred that BB might suppress the excessive release of cytokines induced by PR8 in the A549 cells via blocking the TLR3, p38 MAPK, and PI3K-AKT signaling pathways.

BB Significantly Alleviates PR8-Induced Acute Lung Injury (ALI) in Mice

The anti-inflammatory effects of BB were further validated on PR8-induced ALI in mice given the results that BB could effectively inhibit the inflammatory response triggered by PR8 in vitro. The histopathological results showed that no histological change was observed in the normal group and evident pathological changes such as disappearance of pulmonary alveoli, extensive consolidation, and massive inflammatory cell infiltration, were observed in the lungs of the mice in the model group compared with the normal group. When compared with the model group, intact alveolar space and a decrease in inflammatory cell infiltration were observed in mice treated with BB (500 or 250 mg/kg) (Figure 10A), suggesting that BB (500 or 250 mg/kg) had a significant ameliorating effect on the ALI caused by PR8.

Moreover, the lung index of the mice in the model group was significantly higher ($p < 0.001$) than that in the normal group, indicating that severe pulmonary inflammatory exudate and edema were induced by PR8 in the lung. The lung indices of mice in the BB (500 or 250 mg/kg) group were significantly lower ($p < 0.05$ or $p < 0.01$) than those in the model group (Figure 10B).

Influenza infection could induce an aggressive pro-inflammatory response including excessive release of cytokines and chemokines, which could contribute to pulmonary immunopathology. A significant increase in the mRNA expression levels of cytokines (CXCL1/KC, TNF-α, CXCL9/MIG, and IL-1β) ($p < 0.001$) was observed in the model group, when compared with the normal group. However, the mRNA expression levels of CXCL1/KC, TNF-α, and CXCL9/MIG were significantly down-regulated by the BB group (500, 250, or 125 mg/kg) ($p < 0.001$ or $p < 0.01$ or $p < 0.05$) (Figure 10C–E). In addition, BB (500 and 250 mg/kg) could significantly inhibit the mRNA expression levels of IL-1β ($p < 0.001$) (Figure 10F). In summary, BB could efficiently alleviate the ALI induced by PR8.
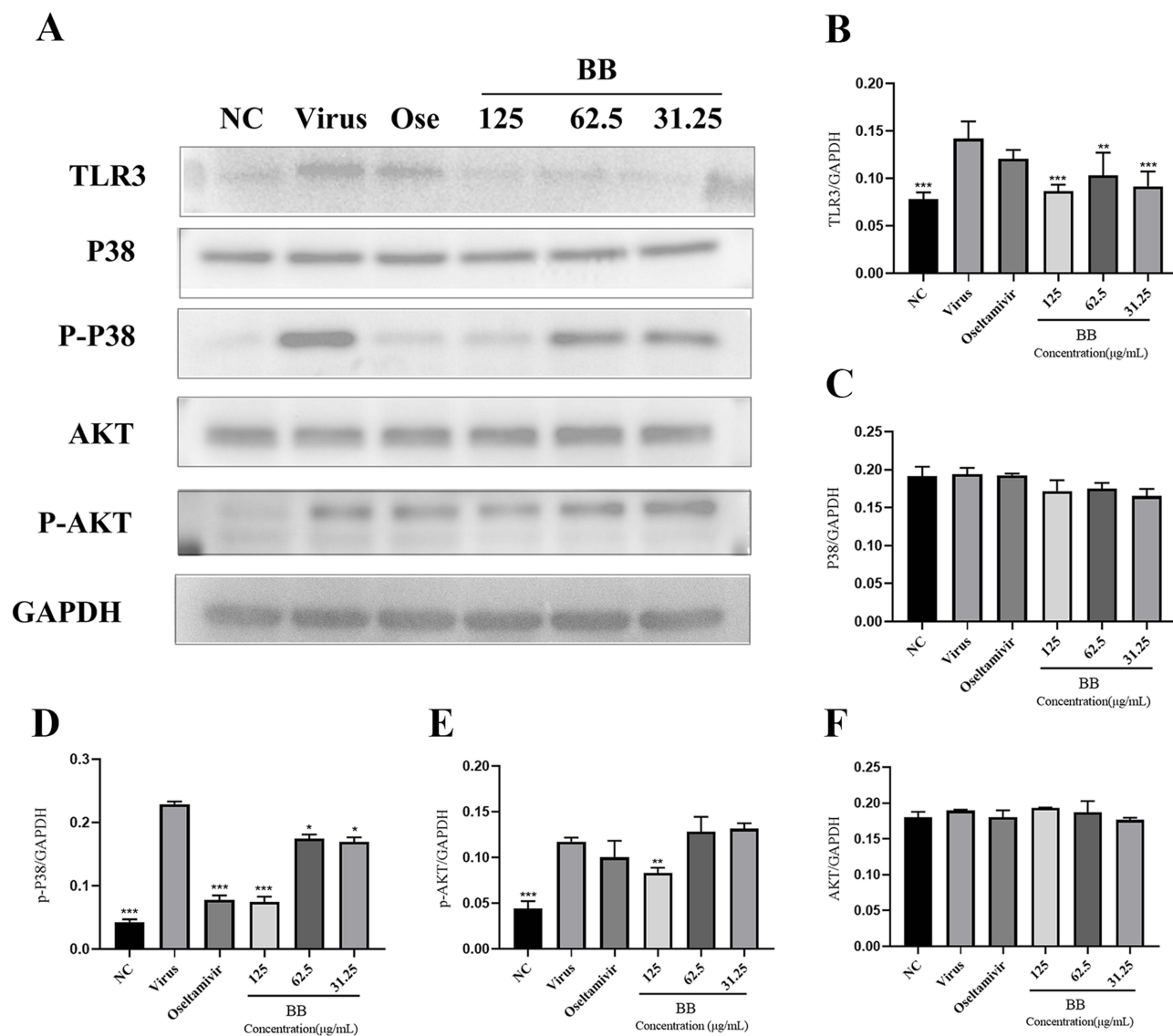
Figure 9 The inhibitory effect of BB (125 μg/mL, 62.5 μg/mL and 31.25 μg/mL) or oseltamivir (20 μM) on regulating the TLR3, p38 MAPK and PI3K- AKT signaling pathways in the A549 cells. (**A**) The expression of the TLR3, p38, p-p38, AKT and p-AKT proteins in the A549 cells was detected by Western blot analysis; (**B–F**) The quantitative analysis of the TLR3, p38, p-p38, AKT and p-AKT proteins was analyzed by Image J. The values were presented as the means ± S.D. of three individual experiments. *$p<0.05$; **$p<0.01$; ***$p<0.001$, when compared to the model group.

Discussion

Influenza virus is one of the most common pathogens that can cause highly contagious severe respiratory diseases and give rise to thousands of deaths each year.[5] Despite the development in the antiviral agents against influenza, the strategies for treatment of influenza virus and the hyperinflammation status caused by influenza virus remain limited. At present, TCMs, especially traditional Chinese formulas, such as lianhua qingwen, have gained extensive attention worldwide on the treatment of respiratory viral infections including SARS-CoV-2 and influenza infection for their benefits to clinical patients.[34] In China, TCMs have been widely used in the treatment of influenza virus infection. At the same time, patients with influenza infection usually benefit from TCMs clinically.[16] Studying the mechanism of TCMs on influenza infection is difficult due to their complex and various ingredients. With the development of comprehensive TCM databases, network pharmacology has been employed as a rational method to study the drug combinations, target prediction, mechanism study and network toxicology research of TCMs via establishing compound-target-disease network, signaling pathway analysis and PPI network construction.[35]
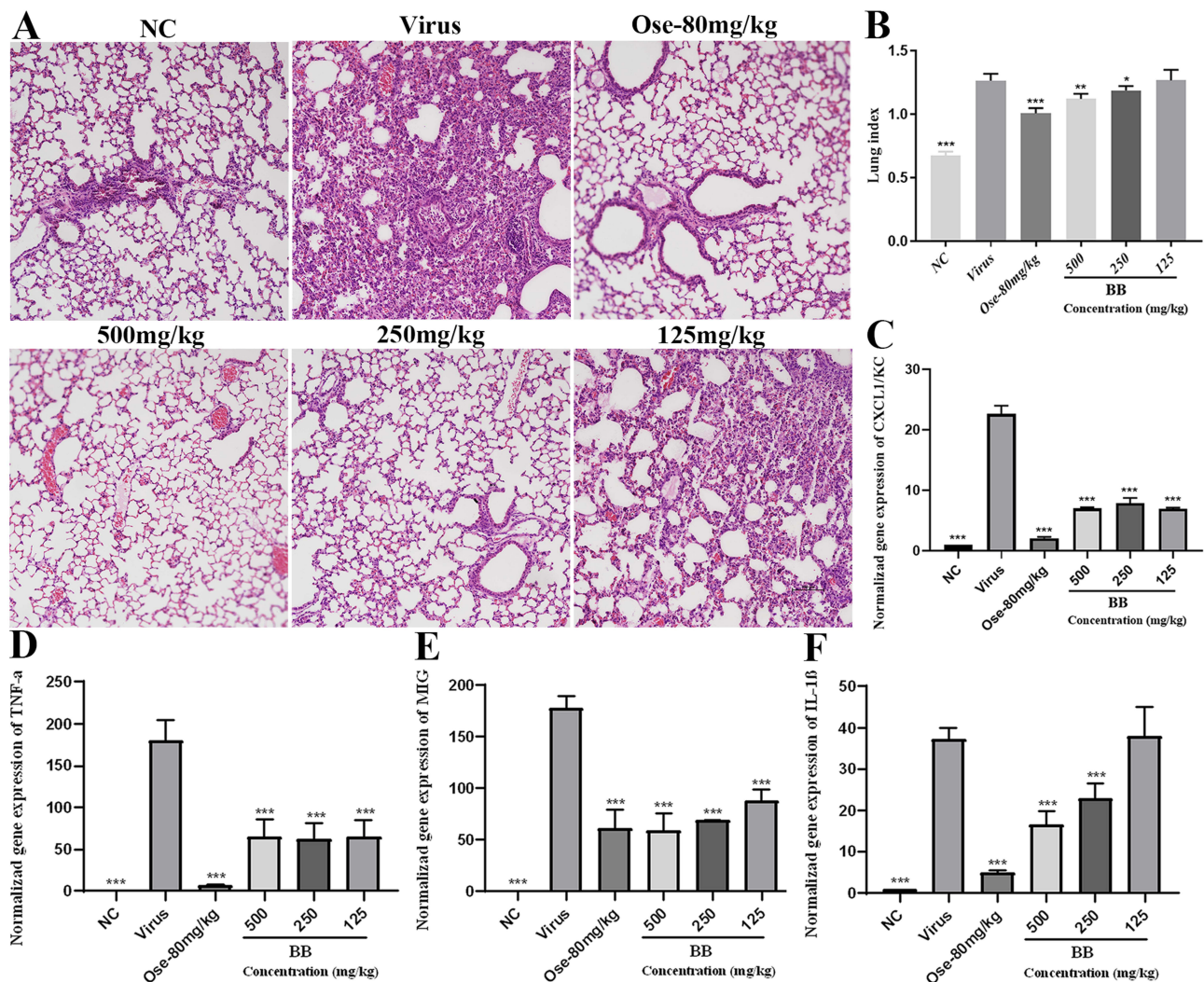
Figure 10 The protective activities of BB on ALI induced by PR8. (**A**) Histological observations of lung tissues for mice sacrificed at the fifth d.p.i. Scale bar = 100 μm; (**B**) Lung index for mice sacrificed at the fifth d.p.i; (**C–F**) The mRNA expression of CXCL1/KC, TNF-α, CXCL9/MIG, IL-1β of the infected mice were detected by RT-qPCR analysis. The values were presented as the means ± S.D. of three individual experiments. *$p<0.05$; **$p<0.01$; ***$p<0.001$, when compared to the model group.

In terms of the complexity of the active components of BB and diversity of potential treatment-targets in humans, a summary of influenza-related target proteins of the compounds in BB were collected from multiple databases for network pharmacology analysis. PPI relationship network and GO and KEGG signaling enrichment analysis were employed to analyze the core targets, potential biological processes and signaling pathways, respectively. GO and KEGG signaling enrichment analysis suggested that BB interfered influenza infection possibly via negative regulation of the apoptotic process. Influenza virus infection could induce cytopathic effects such as apoptosis and necrosis.[36,37] Apoptosis in alveolar epithelial cells caused by influenza virus can destroy the physical epithelial layer and impair the epithelial–endothelial barrier.[36] Destruction of epithelial–endothelial barrier is a major cause of respiratory failure in the acute phase of ARDS.[38] In this study, we confirmed the protective effect of BB in MDCK cells via CPE experiments. Our results indicated that BB could protect cells from virus-induced cell death in vitro. Subsequently, our further experiments suggested that BB could significantly inhibit the apoptotic process induced by PR8 and decrease the expression of classical markers of apoptosis, such as cleaved PARP. Influenza virus can modulate host apoptotic responses to facilitate their own survival, and P38 MAPK is responsible to induce apoptotic cell death caused by influenza virus.[39] Our results showed that BB could inhibit the expression of phosphorylation of p38 protein in A549 cells. These results indicated that BB might suppress influenza virus-induced apoptotic process via downregulation of P38 MAPK signaling pathway.

According to the results of network pharmacology, 153 potential active components against influenza and 194 influenza-related targets were found. Among them, 30 targets and 51 ingredients were involved in influenza signaling pathway by BB. Among these ingredients, the main active ingredients of BB, such as quercetin, kaempferol, and β-sitosterol, have clear anti-inflammatory or antiviral effects against influenza virus. GO and KEGG signaling enrichment analysis suggested that inflammatory response was a key biological process of BB involved in influenza infection. TNF-α, IL-6, IL-1β, MCP-1/CCL-2, CXCL-10/IP-10, C-C motif chemokine 5 (CCL-5/RANTES) and C-X-C motif chemokine 2 (CXCL-2) are key pro-inflammatory genes and MAPK1, mitogen-activated protein kinase 8 (MAPK8), Mitogen-activated protein kinase14 (MAPK14), AKT1, TLR3 and TLR7 are key genes of inflammation-related signaling pathways, to which BB may target. TNF-α can be produced by different cell types including DCs, lung epithelial cells, helper T cells and cytotoxic T lymphocytes after influenza infection, which is considered the prototypical proinflammatory cytokine at the center of the influenza cytokine storm.[40] MCP-1/CCL-2, CXCL-10/IP-10, and CXCL-8/IL-8 can recruit mixed inflammatory cells, such as monocytes, neutrophils, and macrophages, which can cause immunopathology and mortality.[8] TNF-α, IL-6, MCP-1/CCL-2, CXCL-10/IP-10, and CXCL-8/IL-8 have been found to be highly increased and associated with disease severity in influenza infection.[41,42] TLR, MAPK and PI3K-AKT signaling pathways play an important role in regulating the release of pro-inflammatory cytokines.[43] Consequently, in vitro experiments were carried out to determine the anti-inflammatory activities of BB and the potential mechanism. Intriguingly, BB could significantly suppress the mRNA expression of IL-6, CXCL-8/IL-8, CXCL-10/IP-10, TNF-α, and MCP-1/CCL-2 induced by PR8 in A549 cells. Our further experiments inferred that BB could markedly inhibit the protein expression of TLR3 and the phosphorylation of AKT and p38 protein. Moreover, BB alleviated the inflammatory response induced by PR8 probably via blocking TLR3, p38 MAPK or PI3K-AKT signaling pathways. The results of the docking study revealed that kaempferol, β-sitosterol, bufothionine, decamine, and quercetin combined effectively with crucial proteins of TLR, MAPK, and PI3K-AKT signaling pathways. Some studies indicate that kaempferol, β-sitosterol, bufothionine, decamine, and quercetin possess anti-inflammatory activity against influenza virus-induced or LPS-induced inflammation.[28,33,44,45] Therefore, the main possible compounds could be bufothionine, decamine, kaempferol, quercetin, and β-sitosterol, which exert anti-inflammatory effect.

The in vitro experiment cannot fully reflect the effect of BB on influenza infection. A mouse model of PR8-induced pneumonia was constructed to further determine the effect of BB on ALI induced by influenza virus. The lung index and the pathological changes are indicators of the severity of pneumonia in the infected mice. BB (500 and 250 mg/kg) could efficiently improve the pathological changes and significantly reduce the lung index in the lungs of the infected mice, hinting that BB could protect against influenza virus-induced ALI. MCP-1, IL-8 and CXCL1/KC could recruit neutrophils into the infected lung, which destroy normal lung tissues via releasing of reactive oxygen species (ROS) and secretions of proteases.[7] In line with the inhibitory effect of BB on the expression of MCP-1, IL-8 and TNF-α in vitro, our results showed that BB could drastically reduce the mRNA expression of TNF-α and CXCL1/KC in the lungs of the infected mice. Furthermore, BB could also inhibit the expression of CXCL9/MIG and IL-1β in lungs. These results indicated that BB could effectively alleviate ALI induced by PR8 by decreasing the hyper-activated immune response.

Conclusion

In summary, we systematically revealed that BB could improve influenza virus-induced over-activated inflammatory response and apoptosis process via multi-ingredients and multi-proteins based on network pharmacology. Our preliminarily conclusion was that BB could inhibit influenza A virus replication in vitro and ameliorate PR8-induced inflammation possibly via negative regulation apoptosis process and blocking TLR3, p38 MAPK or PI3K-AKT signaling pathways. These findings indicated that BB might be an effective anti-inflammatory agent and could be a new option for the treatment of influenza. Further research will be conducted to investigate the safety and efficacy of the treatment of patients with influenza. In addition, network pharmacology can provide a platform for matching candidate compounds with potential targets to develop safe and new agents for the treatment of influenza.

Data Sharing Statement

The data used to support the findings of this study are available from the corresponding author upon request.

Ethics Approval and Consent to Participate

This animal experiment was approved by the Ethics Committee of Guangzhou Medical University (2021061).

Consent for Publication

The manuscript was approved by all authors for publication.

Funding

Disclosure

All the authors declare that the research was conducted in the absence of any commercial or financial relationships that could be construed as a potential conflict of interest.

References

1. Uyeki TM, Hui DS, Zambon M, Wentworth DE, Monto AS. Influenza. *Lancet*. 2022;400(10353):693–706. doi:10.1016/S0140-6736(22)00982-5
2. Taubenberger JK, Kash JC, Morens DM. The 1918 influenza pandemic: 100 years of questions answered and unanswered. *Sci Transl Med*. 2019;11 (502). doi:10.1126/scitranslmed.aau5485
3. Uyeki TM, Bernstein HH, Bradley JS, et al. Clinical Practice Guidelines by the Infectious Diseases Society of America: 2018 Update on Diagnosis, Treatment, Chemoprophylaxis, and Institutional Outbreak Management of Seasonal Influenza. *Clin Infect Dis*. 2019;68(6):e1–e47. doi:10.1093/cid/ciy866
4. Iuliano AD, Roguski KM, Chang HH, et al. Estimates of global seasonal influenza-associated respiratory mortality: a modelling study. *Lancet*. 2018;391(10127):1285–1300. doi:10.1016/S0140-6736(17)33293-2
5. Wang Y, Fan G, Horby P, et al. Comparative Outcomes of Adults Hospitalized With Seasonal Influenza A or B Virus Infection: application of the 7-Category Ordinal Scale. *Open Forum Infect Dis*. 2019;6(3):ofz053. doi:10.1093/ofid/ofz053
6. Zhou F, Wang Y, Liu Y, et al. Disease severity and clinical outcomes of community-acquired pneumonia caused by non-influenza respiratory viruses in adults: a multicentre prospective registry study from the CAP-China Network. *Eur Respir J*. 2019;54(2):1802406. doi:10.1183/13993003.02406-2018
7. Bermejo-Martin JF, Martin-Loeches I, Rello J, et al. Host adaptive immunity deficiency in severe pandemic influenza. *Crit Care*. 2010;14(5):R167. doi:10.1186/cc9259
8. Alon R, Sportiello M, Kozlovski S, et al. Leukocyte trafficking to the lungs and beyond: lessons from influenza for COVID-19. *Nat Rev Immunol*. 2020;21(1):49–64. doi:10.1038/s41577-020-00470-2
9. Li Z, Li L, Zhao S, et al. Re-understanding anti-influenza strategy: attach equal importance to antiviral and anti-inflammatory therapies. *J Thorac Dis*. 2018;10(Suppl 19):S2248–S2259. doi:10.21037/jtd.2018.03.169
10. Blum CA, Nigro N, Briel M, et al. Adjunct prednisone therapy for patients with community-acquired pneumonia: a multicentre, double-blind, randomised, placebo-controlled trial. *Lancet*. 2015;385(9977):1511–1518. doi:10.1016/S0140-6736(14)62447-8
11. Li C, Yang P, Zhang Y, et al. Corticosteroid treatment ameliorates acute lung injury induced by 2009 swine origin influenza A (H1N1) virus in mice. *PLoS One*. 2012;7(8):e44110. doi:10.1371/journal.pone.0044110
12. Diaz E, Martin-Loeches I, Canadell L, et al. Corticosteroid therapy in patients with primary viral pneumonia due to pandemic (H1N1) 2009 influenza. *J Infect*. 2012;64(3):311–318. doi:10.1016/j.jinf.2011.12.010
13. Ni YN, Chen G, Sun J, Liang BM, Liang ZA. The effect of corticosteroids on mortality of patients with influenza pneumonia: a systematic review and meta-analysis. *Crit Care*. 2019;23(1):99. doi:10.1186/s13054-019-2395-8
14. Dong G, Peng C, Luo J, et al. Adamantane-resistant influenza a viruses in the world (1902–2013): frequency and distribution of M2 gene mutations. *PLoS One*. 2015;10(3):e0119115. doi:10.1371/journal.pone.0119115
15. Lampejo T. Influenza and antiviral resistance: an overview. *Eur J Clin Microbiol Infect Dis*. 2020;39(7):1201–1208. doi:10.1007/s10096-020-03840-9
16. Ma Q, Chen R, Zeng J, et al. Investigating the effects of Liushen Capsules (LS) on the metabolome of seasonal influenza: a randomized clinical trial. *Front Pharmacol*. 2022;13:1. doi:10.3389/fphar.2022.1036927. eCollection 2022
17. Zhang ZJ, Morris-Natschke SL, Cheng YY, Lee KH, Li RT. Development of anti-influenza agents from natural products. *Med Res Rev*. 2020;40 (6):2290–2338. doi:10.1002/med.21707
18. Geng P, Zhu H, Zhou W, et al. Baicalin Inhibits Influenza A Virus Infection via Promotion of M1 Macrophage Polarization. *Front Pharmacol*. 2020;11:01298. doi:10.3389/fphar.2020.01298
19. Zhou B, Liang X, Feng Q, et al. Ergosterol peroxide suppresses influenza A virus-induced pro-inflammatory response and apoptosis by blocking RIG-I signaling. *Eur J Pharmacol*. 2019;860:172543. doi:10.1016/j.ejphar.2019.172543

20. Liang X, Huang Y, Pan X, et al. Erucic acid from Isatis indigotica Fort. suppresses influenza A virus replication and inflammation in vitro and in vivo through modulation of NF-kappaB and p38 MAPK pathway. *J Pharm Anal*. 2020;10(2):130–146. doi:10.1016/j.jpha.2019.09.005

21. Shi Y, Xu H, Xiao Y, et al. Gegen Qinlian Decoction Downregulates the TLR7 Signalling Pathway to Control Influenza A Virus Infection. *Biomed Pharmacother*. 2020;121:109471. doi:10.1016/j.biopha.2019.109471

22. Deng L, Shi Y, Liu P, et al. GeGen QinLian decoction alleviate influenza virus infectious pneumonia through intestinal flora. *Biomed Pharmacother*. 2021;141:111896. doi:10.1016/j.biopha.2021.111896

23. Li Zhan NJ. Clinical study of antelope horn powder on pediatric upper respiratory tract infection. *J Pediatric Tradition Chin Med*. 2011;7(05):12–13.

24. Ma Q, Huang W, Zhao J, Yang Z. Liu Shen Wan inhibits influenza a virus and excessive virus-induced inflammatory response via suppression of TLR4/NF-kappaB signaling pathway in vitro and in vivo. *J Ethnopharmacol*. 2020;252:112584. doi:10.1016/j.jep.2020.112584

25. Yong Q. Clinical observation of Liushen Pill in the treatment of influenza. *Chin Traditional Herbal Drugs*. 2021;52(06):1687–1691.

26. Jinping WP WANG. CHEN Runhua,CHIU Peiyan,HUANG Zeyu,WU Hanwei,WU Jianlong. Effect of hydroxy saffron yellow pigment A on pro/anti-inflammatory factors in peripheral blood of septic mice. *J Sun Yat-Sen Univ*. 2017;38(05):665–669.

27. Yiran WW ZHENG, Xiuwei YANG. Novel butylphthalide derivatives from Chuanxiong that inhibit lipopolysaccharide-induced NO production in RAW264.7 and BV2 cell lines. *Chin Traditional Herbal Drugs*. 2018;49(07):1497–1503.

28. Zhou BX, Li J, Liang XL, et al. beta-sitosterol ameliorates influenza A virus-induced proinflammatory response and acute lung injury in mice by disrupting the cross-talk between RIG-I and IFN/STAT signaling. *Acta Pharmacol Sin*. 2020;41(9):1178–1196. doi:10.1038/s41401-020-0403-9

29. Hu E, Li Z, Li T, et al. A novel microbial and hepatic biotransformation-integrated network pharmacology strategy explores the therapeutic mechanisms of bioactive herbal products in neurological diseases: the effects of Astragaloside IV on intracerebral hemorrhage as an example. *ChinMed*. 2023;18(1):40. doi:10.1186/s13020-023-00745-5

30. Cheng M, Li T, Hu E, et al. A novel strategy of integrating network pharmacology and transcriptome reveals antiapoptotic mechanisms of Buyang Huanwu Decoction in treating intracerebral hemorrhage. *J Ethnopharmacol*. 2024;319(Pt 1):117123. doi:10.1016/j.jep.2023.117123

31. Liu Y, Grimm M, Dai WT, Hou MC, Xiao ZX, Cao Y. CB-Dock: a web server for cavity detection-guided protein-ligand blind docking. *Acta Pharmacol Sin*. 2020;41(1):138–144. doi:10.1038/s41401-019-0228-6

32. Wu W, Li R, Li X, et al. Quercetin as an Antiviral Agent Inhibits Influenza A Virus (IAV) Entry. *Viruses*. 2015;8(1):6. doi:10.3390/v8010006

33. Zhang R, Ai X, Duan Y, et al. Kaempferol ameliorates H9N2 swine influenza virus-induced acute lung injury by inactivation of TLR4/MyD88-mediated NF-kappaB and MAPK signaling pathways. *Biomed Pharmacother*. 2017;89:660–672. doi:10.1016/j.biopha.2017.02.081

34. Hu K, Guan WJ, Bi Y, et al. Efficacy and safety of Lianhua Qingwen capsules, a repurposed Chinese herb, in patients with Coronavirus disease 2019: a multicenter, prospective, randomized controlled trial. *Phytomedicine*. 2022;94:153800. doi:10.1016/j.phymed.2021.153800

35. Xia W, Hu S, Wang M, Xu F, Han L, Peng D. Exploration of the potential mechanism of the Tao Hong Si Wu Decoction for the treatment of postpartum blood stasis based on network pharmacology and in vivo experimental verification. *J Ethnopharmacol*. 2021;268:113641. doi:10.1016/j.jep.2020.113641

36. Uiprasertkul M, Kitphati R, Puthavathana P, et al. Apoptosis and pathogenesis of avian influenza A (H5N1) virus in humans. *Emerg Infect Dis*. 2007;13(5):708–712. doi:10.3201/eid1305.060572

37. Mauad T, Hajjar LA, Callegari GD, et al. Lung pathology in fatal novel human influenza A (H1N1) infection. *Am J Respir Crit Care Med*. 2010;181(1):72–79. doi:10.1164/rccm.200909-1420OC

38. Bonaventura A, Vecchié A, Dagna L, et al. Endothelial dysfunction and immunothrombosis as key pathogenic mechanisms in COVID-19. *Nat Rev Immunol*. 2021;21(5):319–329. doi:10.1038/s41577-021-00536-9

39. Nencioni L, De Chiara G, Sgarbanti R, et al. Bcl-2 expression and p38MAPK activity in cells infected with influenza A virus: impact on virally induced apoptosis and viral replication. *J Biol Chem*. 2009;284(23):16004–16015. doi:10.1074/jbc.M900146200

40. Fajgenbaum DC, Longo DL, June CH. Cytokine Storm. *N Engl J Med*. 2020;383(23):2255–2273. doi:10.1056/NEJMra2026131

41. Bradley-Stewart A, Jolly L, Adamson W, et al. Cytokine responses in patients with mild or severe influenza A(H1N1)pdm09. *J Clin Virol*. 2013;58(1):100–107. doi:10.1016/j.jcv.2013.05.011

42. Betakova T, Kostrabova A, Lachova V, Turianova L. Cytokines Induced During Influenza Virus Infection. *Curr Pharm Des*. 2017;23(18):2616–2622. doi:10.2174/1381612823666170316123736

43. Li X, Shao M, Zeng X, Qian P, Huang H. Signaling pathways in the regulation of cytokine release syndrome in human diseases and intervention therapy. *Signal Transd Target Ther*. 2021;6(1):367. doi:10.1038/s41392-021-00764-4

44. Zhang Y, Takagi N, Yuan B, et al. The protection of indolealkylamines from LPS-induced inflammation in zebrafish. *J Ethnopharmacol*. 2019;243:112122. doi:10.1016/j.jep.2019.112122

45. Sul OJ, Ra SW. Quercetin Prevents LPS-Induced Oxidative Stress and Inflammation by Modulating NOX2/ROS/NF-kB in Lung Epithelial Cells. *Molecules*. 2021;26(22):6949. doi:10.3390/molecules26226949